Mechanism of polyamine induced colistin resistance through electrostatic networks on bacterial outer membranes

Jianguo Li, Roger Beuerman, Chandra S. Verma

PII: S0005-2736(20)30128-0

DOI: https://doi.org/10.1016/j.bbamem.2020.183297

Reference: BBAMEM 183297

To appear in: *BBA - Biomembranes*

Received date: 29 November 2019

Revised date: 21 March 2020

Accepted date: 29 March 2020

Please cite this article as: J. Li, R. Beuerman and C.S. Verma, Mechanism of polyamine induced colistin resistance through electrostatic networks on bacterial outer membranes, *BBA - Biomembranes* (2018), https://doi.org/10.1016/j.bbamem.2020.183297

Mechanism of Polyamine Induced Colistin Resistance through Electrostatic Networks on Bacterial Outer Membranes

Jianguo Li[1*], Roger Beuerman[2,3], Chandra S. Verma[1,4,5,*]

[1]Bioinformatics Institute, A*STAR, 30 Biopolis street, Matrix, Singapore, 138671
[2]Singapore Eye Research Institute, Singapore, 169856, Singapore.
[3]Duke-NUS Graduate Medical School, Eye Academic Clinical Program, Singapore.
[4]National University of Singapore, Department of Biological Sciences, Singapore.
[5]Nanyang Technological University, School of Biological Sciences, Singapore.

Corresponding Authors

* Li Jianguo (lijg@bii.a-star.edu.sg);
* Chandra Verma (chandra@bii.a-star.edu.sg)

Highlights

- Polymyxin B destabilizes the outer membrane of Gram negative bacteria by disrupting the salt-bridges between calcium ions and phosphate groups.
- Naturally occurring linear polyamines can protect the outer membrane against the action of polymyxin B.
- Molecular dynamics simulations revealed the protective mechanism of polyamine through electrostatic networks on bacterial outer membranes.
- Larger polyamines display more significant protective effect on the outer membrane of Gram negative bacteria.

ABSTRACT: Naturally occurring linear polyamines are known to enable bacteria to be resistant to cationic membrane active peptides. To understand this protective mechanism, molecular dynamics simulations are employed to probe their effect on a model bacterial outer membrane. Being protonated at physiological pH, the amine groups of the polyamine engage in favorable electrostatic interactions with the negatively charged phosphate groups of the membrane. Additionally, the amine groups form large number of hydrogen bonds with the phosphate groups. At high concentrations, these hydrogen bonds and the electrostatic network can non-covalently crosslink the lipid A molecules, resulting in stabilization of the outer membrane against membrane active antibiotics such as colistin and polymyxin B. Moreover, large polyamine molecules (e.g., spermidine) have a stronger stabilization effect than small polyamine molecules (e.g., ethylene diamine). The atomistic insights provide useful guidance for the design of next generation membrane active amine-rich antibiotics, especially to tackle the growing threat of multi-drug resistance of Gram negative bacteria.

Graphical Abstract

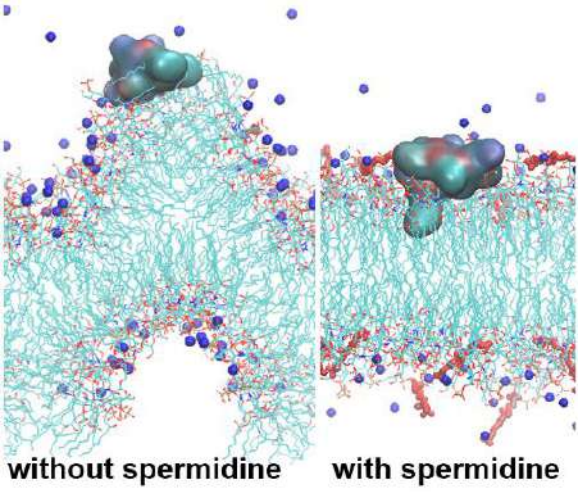

KEYWORDS molecular dynamics simulations; low molecular weight linear polyamine; bacterial outer membrane; colistin; polymyxin B; lipid A

1. Introduction

Bacterial resistance, particularly multi-drug resistance of Gram negative bacteria, has become a critical global health problem [1, 2]. In contrast to Gram positive bacteria, Gram negative bacteria have an additional outer membrane, which poses a high permeation barrier for most hydrophobic antibiotics [3]. Antimicrobial peptides (AMPs) targeting bacterial membranes are promising new generation antibiotics as the membrane is a conservative component of the bacterial cell, thus reducing the chances of resistance arising [4-6]. Colistin is one of the most effective AMPs and functions by disrupting the outer membranes of Gram negative bacteria [7]. However, severe renal toxicity limits the use of colistin to situations when all other antibiotics fail, making it the last resort antibiotic [8]. In recent years, with the rapid increase of multi-drug resistant Gram negative bacterial infections, clinicians have had no choice but to use colistin [7], despite the associated nephrotoxicity.

Colistin belongs to a family of peptides known as polymyxin. Polymyxin peptides consist of a cationic cyclic peptide and an alkyl tail (Figure 1), which enable them to perturb both the head groups and lipid tails of the outer membrane. Colistin differs in only one residue from polymyxin B (PMB), and exerts similar mechanisms of action including displaying a similar antimicrobial spectrum, clinical uses and toxicity [9]. Both colistin and PMB carry 5 positive charges which arise from the amine groups of 5 DAB residues. The antimicrobial activities of colistin and PMB are significantly inhibited by external factors such as divalent cations and some polyamine antagonists [10, 11]. These polyamine antagonists are usually low molecular weight linear polyamines (LMwLPs) consisting of various alkyl and multiple amine groups such as spermidine and spermine (Figure 1). They are found in various eukaryotic and bacterial cells and are known to exhibit multiple biological functions such as porin inhibition, DNA binding, membrane stabilization and response to external stress [12-15]. It has been shown that the presence of LMwLPs (e.g., spermidine) can result in an increase in the MIC of

PMB by up to 16-fold [11, 14]. However, the actual protection of the membranes by LMwLPs remains enigmatic. One mechanism speculated, based on the inhibition of beta-lactam antibiotics, is that LMwLPs can block the porins in the outer membrane, resulting in reduced membrane permeability of the hydrophobic antibiotics[16]. While the inhibition of the porin pathway may partially account for the reduced membrane permeability, it was unable to account for all the experimental observations [11, 13]. Firstly, spermidine and spermine have been shown to reduce the membrane permeability of molecules such as ethidium bromide and acridine orange, whose membrane translocation is porin independent [11]. Secondly, spermidine and spermine have been shown to affect the mechanical properties of membranes, such as increase in the shear modulus of human erythrocyte membranes [17]. Apparently, this enhanced membrane mechanical stability does not result from receptor binding (e.g., porin inhibition), but more likely is mediated by direct interactions of the LMwLPs with lipid molecules [18]. These observations suggest that other mechanisms are at play in the modulation of membrane stability by these LMwLPs.

We carry out computational modelling studies to decipher the molecular mechanism underlying the protective effect of LMwLPs on the stability of the bacterial outer membrane. We choose two model LMwLPs: ethylene diamine (EDA) and spermidine (SPD) (Figure 1). Molecular dynamics (MD) simulations were employed to examine the effects of LMwLPs on the structural properties of a model lipid A (LpA) bilayer that mimics the bacterial outer membrane [19, 20]. Subsequently, PMB was introduced into each system to study how the model LMwLPs attenuates the effects of PMB. Finally, an alternative mechanism of action of these LMwLPs in mediating resistance and associated implications are discussed.

2. Methods:

The main component of the bacterial outer membrane is lipopolysaccharide (LPS), which consists of a lipid A (LpA) portion, an inner core, an outer core and an O-antigen. Each lipid

A molecule is made up of 5-7 lipid tails and an anionic head group, and varies across bacteria. Studies have shown that lipid A is critical for the maintenance of the outer membrane structure [21], making it a good model for studying the molecular mechanisms of outer membrane permeability [22, 23]. In fact, the lipid A portion of the LPS molecule is also the primary target of polymyxins [24]. Using a model of lipid A membrane from *Pseudomonas aeruginosa* bacteria consisting of 64 lipid A molecules that has been used previously (Figure 1) [19, 20], we first simulate the effects of a simple polyamine EDA on the properties of a pure lipid A membrane. In the model lipid A membrane, the head group region of each leaflet of the model lipid A membrane contains 32 calcium ions, so that there is no net electric dipole moment across the membrane. We did not use mono-valent ions such as NaCl or KCl because (i) experimental studies have reported that divalent cations such as calcium or magnesium are required to stabilizes the outer membrane and replacement of divalent cations with monovalent cations results in a permeabilization of the outer membrane [20, 25-27]; (ii) a simulation study has shown that replacement of calcium ions with sodium ions results in a transition from the lamellar to a nonlamellar phase [20]. The effects of EDA were explored by systematically varying its concentrations using EDA/LpA ratios of 0/64, 8/64, 16/64 and 32/64. In each simulation, an equal number of EDA molecules were placed near the two surfaces of a membrane and solvated with water molecules. Additional counter ions were subsequently added to neutralize the system. The system was first relaxed by subjecting it to 500 steps of energy minimization. Next 100 ps of molecular dynamics (MD) simulations were carried out to relax the water molecules. Finally, each system was subject to 1000 ns of production MD simulations. During each simulation, the EDA molecules were observed to be rapidly absorbed onto the two surfaces of the membrane. Following this, the PMB was introduced to the membrane and was placed close to the membrane containing EDA molecules. The system was then solvated and neutralized by additional counter ions. An

energy minimization of 500 steps of gradient descent was carried out, followed by 100 ps of MD simulations to relax the water molecules. For each system, 1000 nanoseconds of production MD simulations were then carried out for each system containing different numbers of EDA molecules. To understand the effects of the molecular size of the polyamine, we also simulated spermidine (SPD) with the model lipid A membrane; the protocol adopted was the same as that employed for the EDA-membrane simulations except that the simulations of SPD with lipid A membrane in the presence of PMB were extended to 2000 nanoseconds; all simulation details are summarized in Table S1. In all simulations, the Gromos53a6 force field was used for EDA, PMB and SPD molecules [28, 29]. For EDA and SPD, the partial atomic charges and dihedral terms were obtained from the ATB server [30], while the bond and angle parameters were taken from the standard GROMOS53a6 force field. For PMB, the partial charges of the unnatural amino acid were obtained by analogy with standard residue charges in the GROMOS force field (e.g., DAB residues vs. LYS), and the bonded parameters were obtained taken from the standard GROMOS force field parameters. The lipid A parameters were taken according to the study of Pontes et al., which were parameterized to be compatible with the GROMOS force field [20]. The SPC model was used to describe water molecules [31]. The LINCS algorithm was used to constrain the bonds between hydrogen atoms and any heavy atoms, which enables a time step of 2 fs to be used in all simulations [32]. A cutoff of 1.4 nm was used to calculate the Lennard-Jones and short range electrostatic interactions. For the long range electrostatic interactions, a reaction field (RF) method with a permittivity dielectric constant of 66 was used, which is compatible with the GROMOS force field used in this study [20, 28, 29]. As the electrostatic interactions play important role in modulating the structure of the lipid A membrane, we also carried out additional control simulations using PME for electrostatic calculations (Table S1). All simulations were carried out in the NPT ensemble with semi-isotropic pressure coupling. The

temperature and pressure were maintained at 300K and 1 bar, respectively. The GROMACS 4.5 package was employed to carry out all the simulations and to perform the analyses [33].

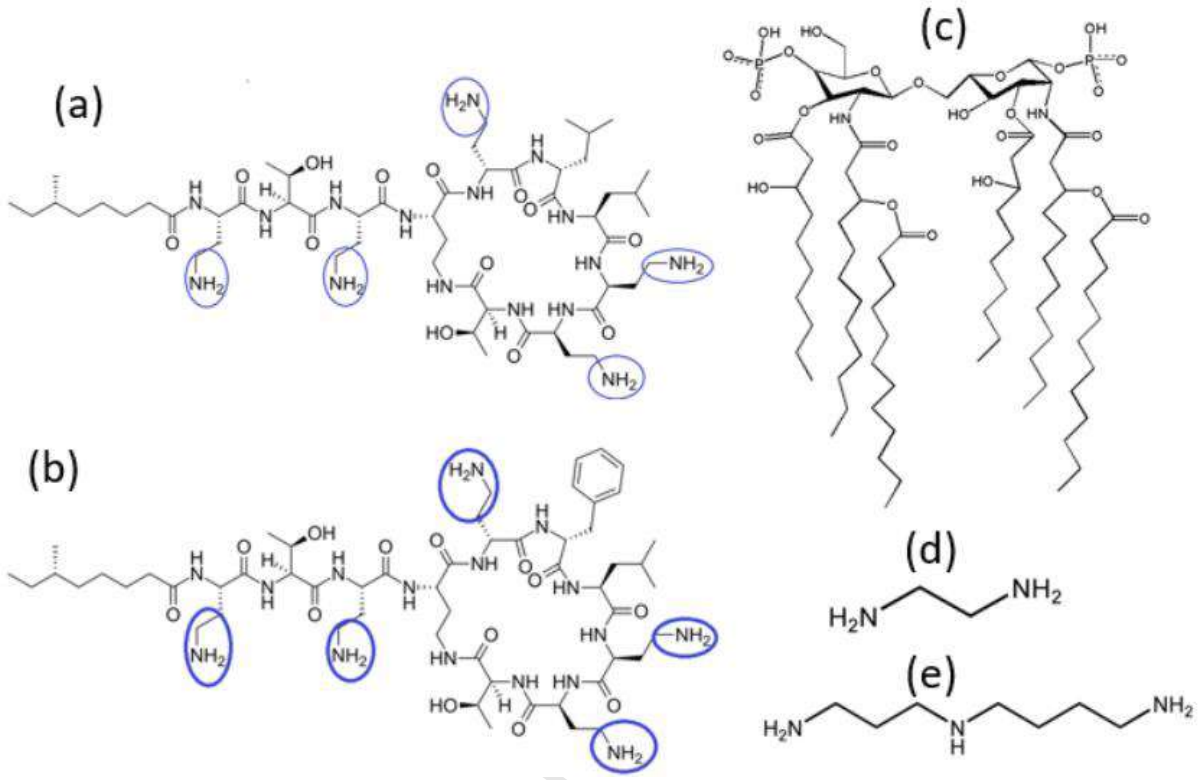

Figure 1. The chemical structures of (a) colistin; (b) polymyxin B; (c) lipid A from *Pseudomonas Aeruginosa*; (d) ethylene diamine and (e) spermidine; the sidechains of the DAB residues are highlighted by blue circles.

3. Results and Discussions

3.1. Mode of interaction of LMwLP with lipid A membranes

To understand the effect of LMwLPs on the structural properties of the normal Gram negative outer membrane, we performed MD simulations of a model lipid A membrane without LMwLP and with different ratios of LMwLP/LpA, corresponding to different LMwLP concentrations. We calculated the distributions of phosphate atoms, the oxygen atoms connecting the head groups with the lipid tails, the water molecules, the calcium ions and the LMwLP molecules for each bilayer (Figure 2). For pure lipid A membrane and the lipid A membrane with either EDA or SPD, the distributions of phosphate groups, the oxygen

atoms and the water molecules display symmetric peaks, which correspond to the two leaflets of the membrane, suggesting that the membrane structure is stable. The overlap between the peak of calcium ions and that of phosphate groups suggests favorable interactions. Indeed, calcium ions and phosphate groups form large numbers of salt-bridges that stabilize the lipid A membrane. It has been reported that removal of divalent cations results in destabilization of the outer membrane [25, 27]. The distributions of EDA/SPD molecules also overlaps with the peaks of the distributions of the phosphate groups, suggesting favorable interactions with the phosphate groups of the membrane. At physiological pH, both EDA and SPD are positively charged; therefore the adsorption of EDA/SPD on to the membrane surface is largely driven by electrostatic interactions. As the EDA/SPD concentration increases (e.g., in the case when EDA/LpA=1/2 or SPD/LpA=1/4), the peak of the distribution of calcium decreases and becomes broad, suggesting that the adsorbed calcium ions are replaced by the EDA/SPD molecules and are released from the membrane surface into the bulk water, as can be seen from the snapshots of the systems for higher EDA/SPD concentrations (Figure S1); figures 2h and 2i also reveal similar observations. For both EDA and SPD, as the concentration increases, the distribution of calcium ions becomes wider and the height of the calcium peak decreases, suggesting more calcium ions are released at higher EDA/SPD concentrations; our findings are consistent with potentiometric experiments which demonstrate that LMwLPs induce calcium release in a concentration dependent manner [34]. This suggests that LMwLP molecules compete with calcium in the interactions with the phosphate groups. Figure 2j shows that at the same concentration (e.g., LMwLP/LpA=1/4), the peaks of SPD for the bulk calcium ions (e.g., at -4 and 4 nm) is higher, suggesting that SPD induces more calcium release than EDA, and this is also consistent with potentiometric measurements demonstrating that more calcium is released in the presence of larger LMwLPs compared to smaller LMwLPs [34]. In addition to the changes in the interactions between head groups, the

adsorption of EDA/SPD on to the membrane surface also affects the overall packing of the lipid molecules. Figure S2 shows the area per lipid of the membrane at different EDA/SPD concentrations. In the presence of EDA/SPD, the area per lipid of the membrane slightly decreases, indicating a closer packing of the lipid molecules. This may enhance the stability of the membrane against external mechanical stress [35, 36].; At low EDA/SPD concentrations (e.g., EDA/LpA=1/8 or SPD/LpA=1/16), the area per lipid decreases significantly because the membrane is distorted and the simulation box in the xy plane shrinks, and this results in underestimation of the actual area per lipid.

Although both LMwLP molecules and calcium ions are positively charged and can mediate favorable electrostatic interactions with phosphate groups, the amine groups of EDA/SPD molecules can engage in additional hydrogen bonds with the phosphate groups, thus resulting in stronger binding affinity of EDA/SPD for the phosphate groups. Figure 3 shows the radial distribution function (RDF) between the amine groups of EDA/SPD molecules and the phosphate groups of the membrane. All the systems display high peaks at 0.39 nm, and the cumulative number increases with the LMwLP/LpA ratio, suggesting increased electrostatic interactions between the amine and phosphate groups. This results in an electrostatic network that counteracts the repulsion between negatively charged lipid A molecules. Figure 3 also revealed that at identical LMwLP/LpA ratios (e.g., 1/8 or 1/4), the cumulative number is higher for SPD than for EDA, suggesting that SPD can crosslink more phosphate groups than EDA can. As noted above, adsorption of EDA/SPD induces calcium release. To investigate this, the RDF of calcium ions with respect to the phosphate groups was calculated (Figure S3). The first peak of the RDF at 0.33 nm corresponds to tightly bound calcium ions and increases at low LMwPL concentrations (e.g., EDA/LpA=1/4 and SPD/LpA=1/16). However, the peak at 0.53 nm corresponding to loosely bound calcium ions decreases with the EDA/SPA concentration. On the other hand, the cumulative number of calcium ions

around the phosphate groups for low EDA/SPD concentration (e.g., EDA/LpA=1/8 and SPD/LpA=1/16) is similar to that seen for the pure membrane, but significantly decreases at high EDA/SPD concentration (e.g., EDA/LpA>=1/4 or SPD/LpA>=1/8). These results suggest that EDA/SPD largely replace the calcium ions that are loosely bound to the membrane. To further understand how EDA/SPD replace the membrane bound calcium ions, we calculated the diffusion coefficient of the calcium ions close to the phosphate groups of the membrane (Table S2). We found that only few calcium ions remain in the membrane-bound state throughout the entire simulation, and the rest of the calcium ions undergo an adsorption-desorption-adsorption process. To minimize the statistical error, we divided the last 500 ns of each simulation into 5 blocks so that in each 100 ns block there are more number of calcium ions bound to the phosphate groups. Table S2 shows that the diffusion coefficient of bound calcium ions with respect to the lipid molecules is high for pure membrane, and decreases as the EDA/SPD concentration increases, suggesting that the loosely bound calcium are more easily replaced by EDA/SPD. In addition, the hydration of the phosphate group was examined using the RDF of water molecules with respect to the phosphate groups (Figure S4). In all the RDFs, the first peak of water decreases as the EDA/SPD concentration increases, suggesting reduced hydration of the phosphates upon adsorption of the EDA/SPD.

The total number of hydrogen bonds between EDA/SPD and the phosphate groups were also calculated (Figures 4a and 4b). As the EDA/SPD concentration increases, the total number of hydrogen bonds increases, despite the average number of hydrogen bonds per LMwLP molecules remaining the same (Figures 4c and 4d). When sufficient numbers of hydrogen bonds are formed, the phosphate groups are non-covalently crosslinked by a hydrogen bond network, which further stabilizes the lipid A bilayer. At the same LMwLP/LpA ratio (e.g., 1/4), SPD forms more number of hydrogen bonds with the

phosphate groups than does EDA (Figures 4a and 4b). This is also seen from the average number of hydrogen bonds per LMwLP molecule (Figures 4c and 4d), suggesting that SPD can crosslink more lipid A molecules. Together, the simulations indicate that SPD has a stronger stabilization effect on the lipid A membrane than does EDA. This occurs because SPD contains three amine groups, while EDA contains only two amine groups, resulting in greater calcium release, more hydrogen bonds with phosphate groups and stronger crosslinking of the lipid A molecules in the presence of SPD.

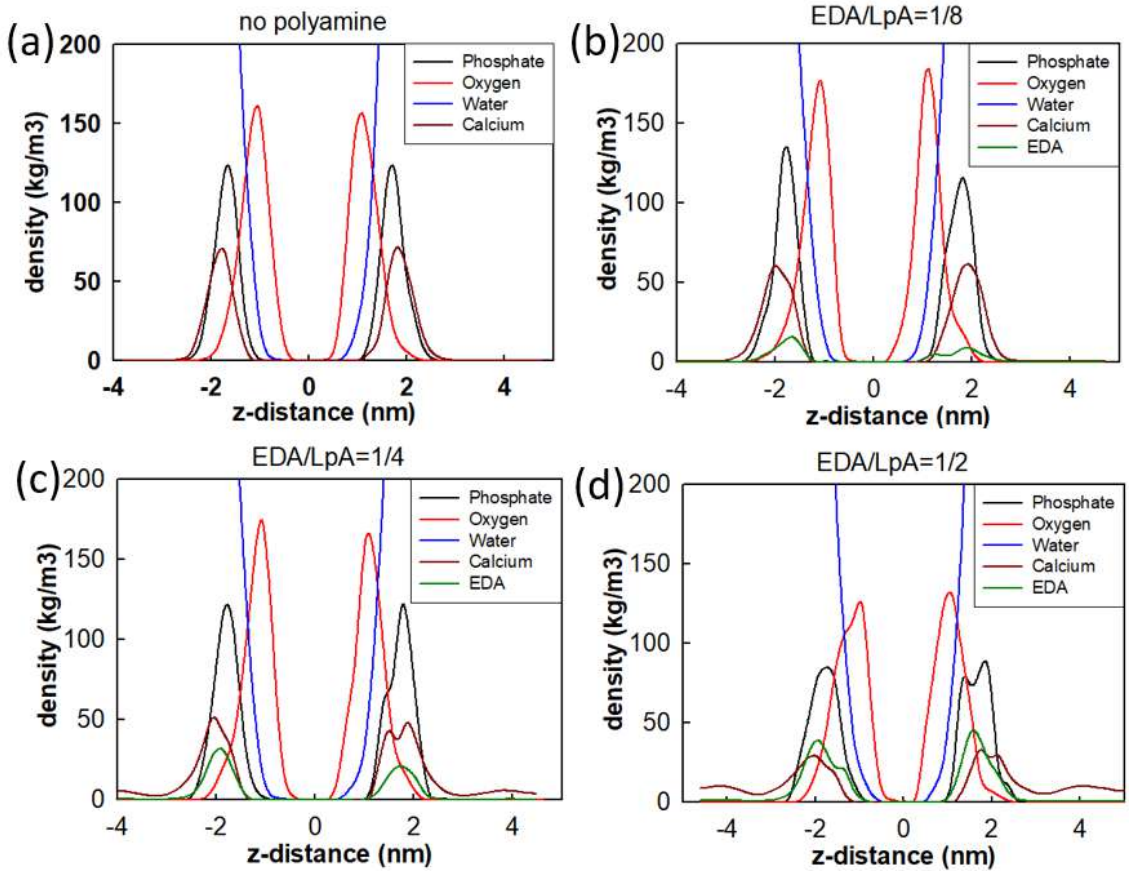

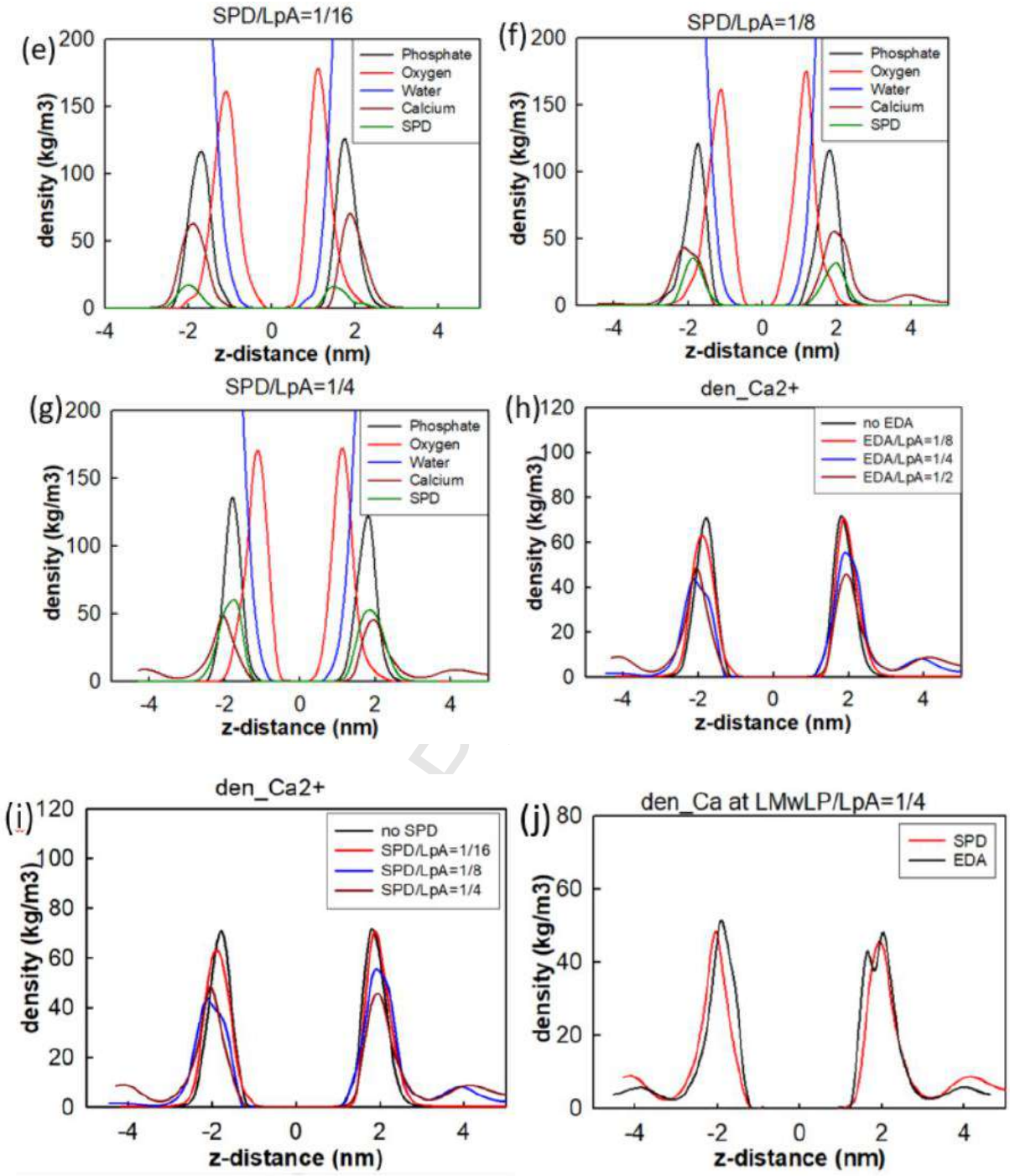

Figure 2. Density distributions of representative groups of the lipid A membrane in the presence of different concentrations of ethylenediamine (EDA) and spermidine (SPD). (a) is for pure lipid A membrane; (b-d) correspond to different EDA/LpA ratios; (e-g) correspond to different SPD/LpA ratios; (h-i) show the calcium distributions for different EDA and SPD concentrations; and (j) compares the calcium distribution of EDA and SPD at LMwLP/LpA ratio of 1/4. The analysis is based on the last 500 ns of each simulation.

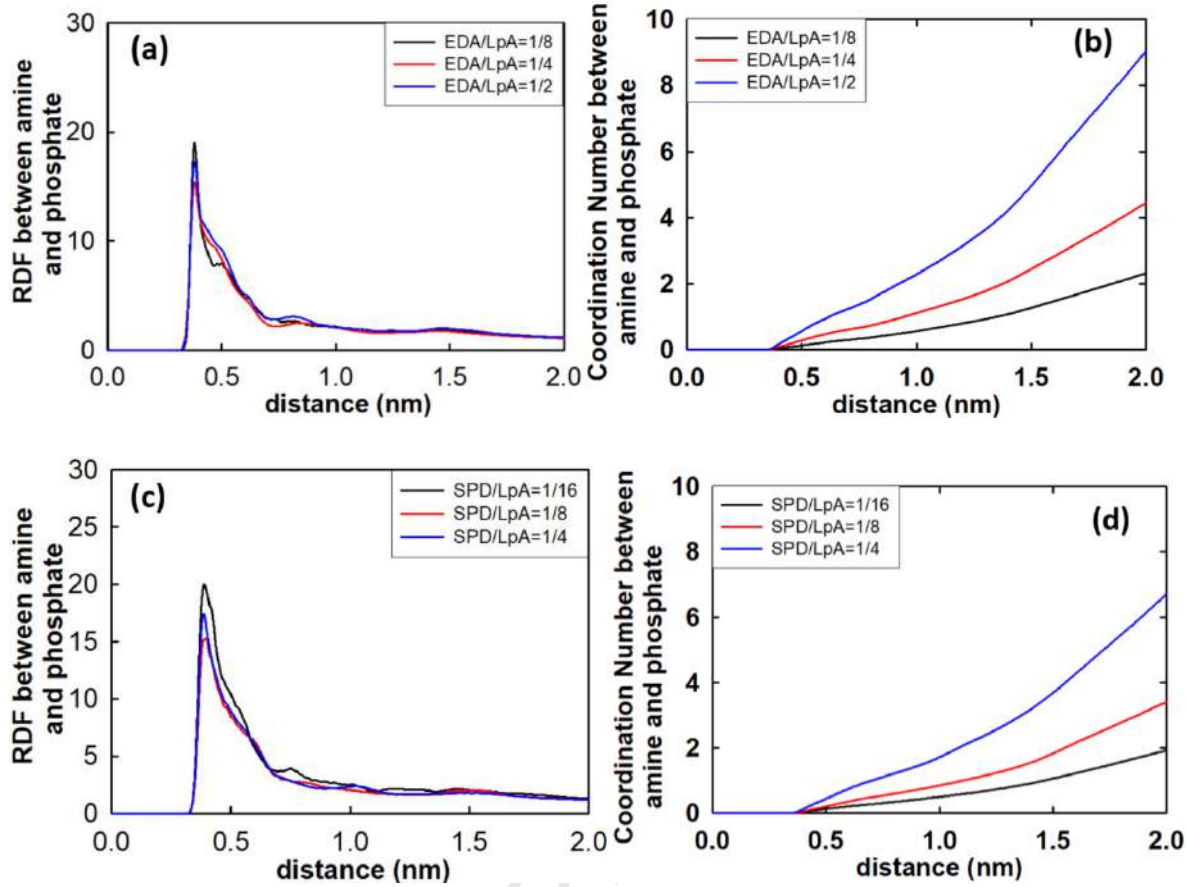

Figure 3. Radial distribution functions (RDF) and the corresponding cumulative numbers of amine groups of LMwLP with respect to the phosphate groups of lipid molecules. (a-b) for EDA; (c-d) for SPD. The analysis is based on the last 500 ns of each simulation.

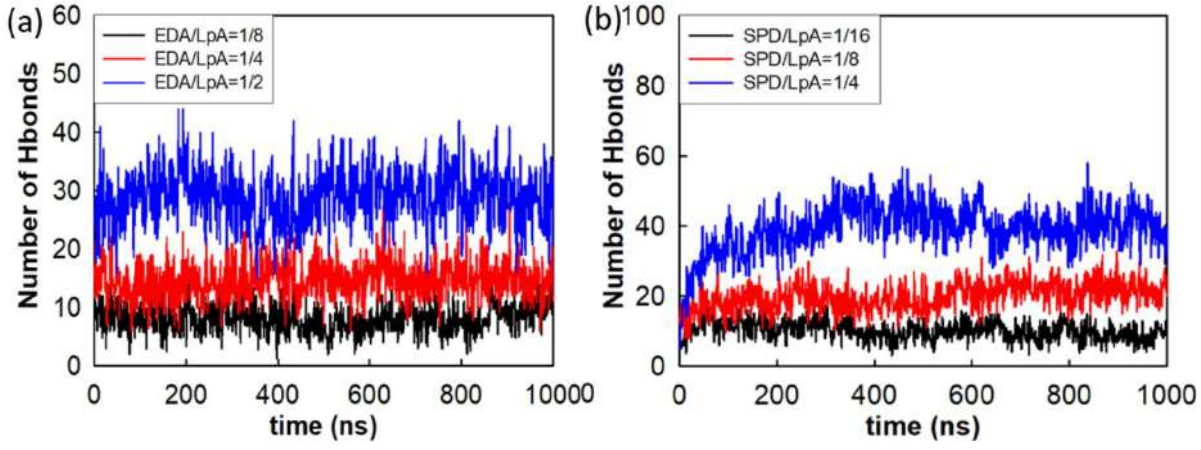

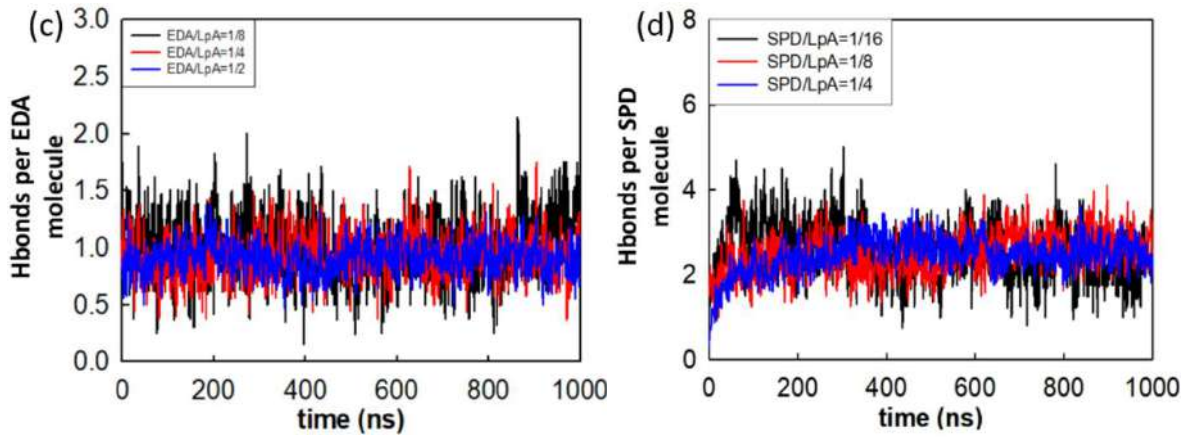

Figure 4. (a-b) Total number of hydrogen bonds between LMwLP and the phosphate groups of the membrane; (c-d) Number of hydrogen bonds per EDA/SPD molecule.

3.2. LMwLP protects the lipid A membrane against the action of PMB

To examine how EDA and SPD modulate the interactions of PMB with the lipid A membrane, we simulated PMB peptide with the model lipid A membranes in the presence of different numbers of EDA/SPD molecules. Three EDA concentrations were simulated, e.g., EDA/LpA=1/8, 1/4 and 1/2; while for SPD, the concentrations examined were SPD/LpA=1/16, 1/8 and 1/4. In the absence of LMwLP molecules, the amine groups of the PMB preferentially interact with the phosphate groups via electrostatic interactions and hydrogen bonding interactions, resulting in the disruption of the salt-bridges and release of calcium ions from the membrane surface (Figure 5). As PMB is an amphiphilic molecule, the hydrophobic moieties further perturb the membrane via hydrophobic interactions, resulting in lipid defects, which allow water to penetrate into the membrane. Altogether, the membrane undergoes significant deformations, which is consistent with the previous observations of the effect of cationic peptides on outer membrane stability [19, 37].

In the presence of both PMB and low concentrations of EDA or SPD molecules, (e.g., EDA/LpA=1/8 or SPD/LpA=1/16), we observed membrane deformations similar to that seen in the absence of EDA (Figure 5 and simulation movies 1 and 2 in the Supplementary

Materials). However, when the EDA/LpA ratio reaches 1/4 and above or the SPD concentration is 1/8 and above, the membrane is stable during the entire simulations, demonstrating resistance to the action of PMB (Figure 5 and simulation movies 3 and 4 in the Supplementary Materials). This suggests that the PMB induced membrane deformation depends on the EDA/SPD concentration and a critical ratio between 1/8 to 1/4 for EDA and 1/16 to 1/8 for SPD is needed to stabilize the lipid A membrane against the action of PMB. The concentration dependence of EDA/SPD induced membrane stabilization suggests favorable interactions of EDA/SPD with lipid A, such as the electrostatic interactions and the hydrogen bonding interactions between the amines and the phosphate groups. When the EDA or the SPD concentration is low, the degree of electrostatic neutralization is low and there are not enough hydrogen bonds that are able to crosslink the lipid A together to resist the action of PMB. In contrast, higher EDA or SPD concentrations favor strong electrostatic neutralization and sufficient numbers of hydrogen bonds can crosslink the lipid A, resulting in stabilization of the lipid A membrane through the extensive electrostatic network against the action of PMB. In the case of high EDA/SPD concentrations (e.g., EDA/LpA=1/2 or SPD/LpA=1/4), the PMB molecule can still interact with the phosphate groups and replace the calcium ions, but the membrane is stabilized by the extensive EDA/SPD induced lipid crosslinking. For example, at SPD/LpA=1/4, the lipid tail of PMB inserts into the hydrophobic region of the membrane. However, this is not sufficient to induce significant membrane deformations as the head groups are stabilized by an electrostatic carpeting emerging from the presence of SPD.

Comparing the destabilization effects of EDA and SPD, the minimum LMwLP/LpA ratio that is required to stabilize the lipid A membrane against the action of PMB is lower for SPD than for EDA, suggesting that SPD is more efficient than EDA in stabilizing the lipid A membrane. For example, at LMwLP/LpA ratio of 1/8, EDA is unable to protect the lipid A

membrane against the action of PMB, while SPD can. This clearly results from the 3 amine groups in SPD compared to the 2 in EDA; the additional amine group results in stronger electrostatic interactions with the head groups of lipid A molecules and the formation of a wider network of hydrogen bonds between the amine groups and the phosphate groups of lipid A, i.e., a more robust electrostatic network.

The above results suggest that the protective mechanism of EDA or SPD originates from electrostatic interactions and hydrogen bonds (e.g., the short range electrostatic interactions), thus highlighting the importance of choosing an appropriate model for simulating the electrostatic interactions. We have used the RF method in the above simulations, but we additionally carried out MD simulations using the PME method for pure lipid A membrane and lipid A membranes in the presence of high and low EDA/SPD concentrations. (e.g., pure membrane with 64 lipid A molecules, membrane of 64 lipid A molecules with 4 SPD, 16 SPD, 8 EDA and 32 EDA molecules, respectively, as shown in Table S1). The density distribution, the RDF, the area per lipid and the hydrogen bonds are shown in Supplementary Materials Figures S5-S14. The results obtained from the simulations using PME are consistent with the results obtained using the RF, with minor differences. The area per lipid of pure lipid A membrane from PME is slightly smaller than that from RF. However, in the presence of SPD or EDA, the area per lipid is essentially the same between the two representations of electrostatics. In addition, the number of hydrogen bonds between SPD and membrane is smaller using PME than using RF. The average number of hydrogen bonds per SPD molecule is about 2 using RF, while it is about 1.5 using PME (Figures 4d and S9d). We carried out additional simulations of lipid A membrane in the presence of both LMwLP and PMB. We observed that under both electrostatic models, the lipid A membrane is unstable at low LMwLP concentrations (e.g., EDA/LpA=1/8 and SPD/LpA=1/16), but is stable when the LMwLP concentration is high (e.g., EDA/LpA=1/2 and SPD/LpA=1/4). Thus

together these simulations suggest that both RF and PME yield similar results and suggest the same underlying mechanism namely, electrostatic interactions between LMwLP and head groups of lipid A (e.g., in the form of H-bonds) can crosslink the head groups of lipid A, which stabilizes the membrane against the action of PMB.

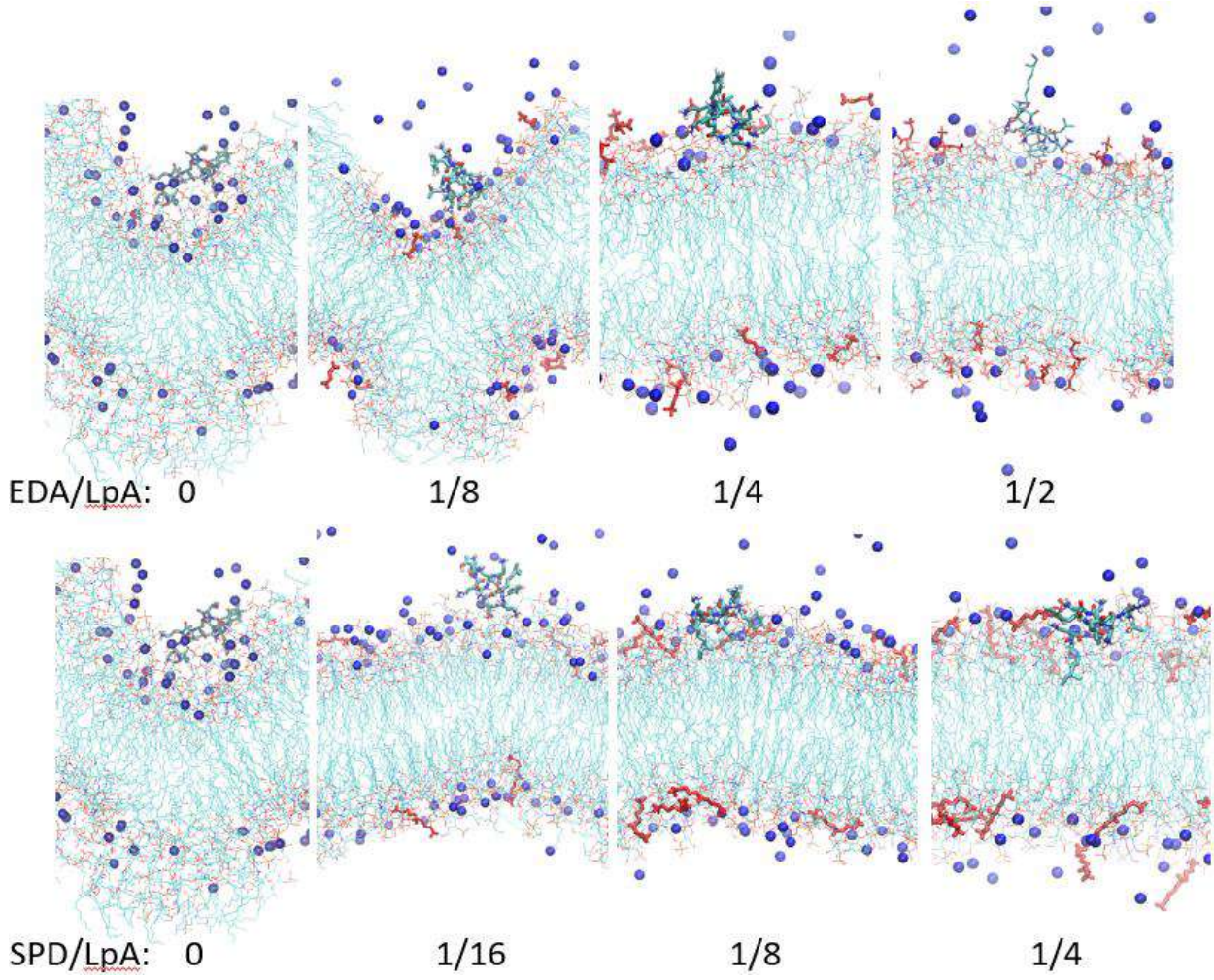

Figure 5. Snapshots of the membrane in the presence of one PMB molecule and different LMwLP/LpA ratios. The blue spheres represents the calcium ions; the sticks represents the PMB molecule and the EDA/SPD molecules are in red color.

4. Implications

In some Gram negative bacteria, the outer membranes contain high concentrations of LMwLPs, constituting a high percentage of the total polyamines in the bacterial cells. It is

possible that these bacteria have evolved to utilize these LMwLPs to protect their outer membranes from external chemical stresses [13, 15, 38]. Moreover, some bacteria can even covalently incorporate amine groups in the head groups of the outer membranes to counteract the action of PMB. For example, in the outer membrane of some PMB resistant bacteria, the lipid A molecule is modified by the covalent attachment of a phosphoethanolamine (PE) group [39]. Similar to the protective LMwLPs studied here, the amine group of PE can electrostatically interact with and form hydrogen bonds with adjacent phosphate groups of another lipid A, resulting in an extensive inter-lipid hydrogen bond network (electrostatic network) that crosslinks the lipid A molecules together. For these bacteria, even if PMB replaces the divalent cations, the membrane is still stabilized by the inter-lipid hydrogen bond network. This mechanism of PMB resistance has become a great challenge for the treatment of Gram negative multi-drug resistant infections. Recently, there has emerged a PMB resistant mutation that is mediated by a mobile plasmid, which has further exacerbated the situation [40, 41].

The MD simulations of PMB and LMwLPs with the model bacterial outer membrane presented in this study provide useful starting points for the design of new amine-rich antimicrobials targeting bacterial membranes. It is interesting that amine-rich molecules can be either membrane protective (e.g., LMwLPs) or membrane disruptive (e.g., PMB and several cationic antimicrobial peptides). This poses a question: what is the role of the amine group in these two classes of molecules with contrasting membrane effects. There are two main structural differences between PMB and LMwLPs. Firstly, PMB is much larger than the LMwLPs. The molecular size is important as large molecules can engage a larger interacting surface of the membrane. For example, the low molecular weight polyamines such as EDA are membrane protective, but high molecular weight polymer forms of EDA (e.g., polyethyleneimine) are excellent outer membrane permeabilizers [42]. Additionally, the PMB

molecule contains many hydrophobic residues and has an amphiphilic structure. Upon adsorption onto the outer membrane, the amine groups of PMB can favorably interact with the phosphate groups of the membrane, but at the same time, the hydrophobic moieties of PMB can insert into the lipid tail region of the membrane, resulting in perturbation of the hydrophobic-water interface of the membrane. Therefore, the presence of large hydrophobic moieties is required for membrane disruption. The lack of large hydrophobic moieties enables LMwLPs such as spermidine to only crosslink the lipid head groups without hydrophobic interference, resulting in stabilization of the membrane. This is consistent with the experimental observation that only molecules with large hydrophobic moieties incorporated with multiple amine groups display outer membrane permeabilization properties, and combination of smaller hydrophobic groups with multiple amine groups has no effect on the permeability of the bacterial outer membrane [34, 43]. In summary, whether the amine rich molecule protects or destabilizes the bacterial outer membrane depends on factors such as the molecular size, the presence of large hydrophobic moieties in the molecule, the charge distribution and the amphiphilicity of the molecule.

5. Conclusions

In summary, our simulations have revealed a new mechanism underlying the protective effect of LMwLPs on the bacterial outer membrane. In the bacterial outer membrane without LMwLPs, the negatively charged lipid A forms salt-bridges with divalent cations such as calcium ions. Upon adsorption on to the bacterial outer membrane, LMwLPs can engage in electrostatic and hydrogen bonding interactions with the negatively charged phosphate groups, resulting in the release of calcium ions into the aqueous phase. The replacement of calcium ions by amine groups also suggests that the amine group has higher affinity compared to the calcium ions for the phosphate groups. Indeed, calcium release in the presence of LMwLPs has been observed in experiments using ion sensitive electrodes [34].

At sufficient concentrations, LMwLPs create an extensive hydrogen bond network that crosslinks the head group of the lipid A together, resulting in resistance to the action of PMB. Moreover, the protective effect is more significant for larger LMwLPs. For example, SPD, with three amine groups, appears to protect the bacterial outer membrane at concentrations that are lower than the concentrations of EDA required to elicit similar effects. Because of a more robust electrostatic network, larger LMwLPs may also affect macroscopic properties such as the mechanical stability of the membrane. Indeed, spermidine has been shown to increase the shear modulus of human erythrocyte membranes [17].

Supplementary Materials

Simulation details, snapshots of lipid A membrane in the presence of different number of LMwLPs, simulation results using PME, simulation movies for systems containing lipid A membrane, PMB and EDA/SPD, and other supplementary figures.

Acknowledgements: The authors would like to thank BII, A*STAR ACRC and NSCC for providing computing resources.

Notes:

Chandra S Verma is founder director of SiNOPSEE Therapeutics; Roger Beuerman is founder of SINSA Labs, this work has no conflict with the two companies.

References

[1] D.I. Andersson, D. Hughes, Antibiotic resistance and its cost: is it possible to reverse resistance?, Nature Reviews Microbiology, 8 (2010) 260.
[2] L.M. Weiner, A.K. Webb, B. Limbago, M.A. Dudeck, J. Patel, A.J. Kallen, J.R. Edwards, D.M. Sievert, Antimicrobial-Resistant Pathogens Associated With Healthcare-Associated Infections: Summary of Data Reported to the National Healthcare Safety Network at the Centers for Disease Control and Prevention, 2011–2014, Infection Control & Hospital Epidemiology, 37 (2016) 1288-1301.
[3] H. Nikaido, Molecular Basis of Bacterial Outer Membrane Permeability Revisited, Microbiology and Molecular Biology Reviews, 67 (2003) 593-656.
[4] C.D. Fjell, J.A. Hiss, R.E.W. Hancock, G. Schneider, Designing antimicrobial peptides: form follows function, Nature Reviews Drug Discovery, 11 (2011) 37.

[5] H.D. Thaker, A. Som, F. Ayaz, D. Lui, W. Pan, R.W. Scott, J. Anguita, G.N. Tew, Synthetic mimics of antimicrobial peptides with immunomodulatory responses, J Am Chem Soc, 134 (2012) 11088-11091.
[6] R.E.W. Hancock, H.-G. Sahl, Antimicrobial and host-defense peptides as new anti-infective therapeutic strategies, Nature Biotechnology, 24 (2006) 1551-1557.
[7] M.E. Falagas, S.K. Kasiakou, L.D. Saravolatz, Colistin: The Revival of Polymyxins for the Management of Multidrug-Resistant Gram-Negative Bacterial Infections, Clinical Infectious Diseases, 40 (2005) 1333-1341.
[8] H. Spapen, R. Jacobs, V. Van Gorp, J. Troubleyn, P.M. Honoré, Renal and neurological side effects of colistin in critically ill patients, Ann Intensive Care, 1 (2011) 14-14.
[9] A. Kwa, S.K. Kasiakou, V.H. Tam, M.E. Falagas, Polymyxin B: similarities to and differences from colistin (polymyxin E), Expert Review of Anti-infective Therapy, 5 (2007) 811-821.
[10] B.A. Newton, Reversal of the Antibacterial Activity of Polymyxin by Divalent Cations, Nature, 172 (1953) 160-161.
[11] D.H. Kwon, C.-D. Lu, Polyamines induce resistance to cationic peptide, aminoglycoside, and quinolone antibiotics in Pseudomonas aeruginosa PAO1, Antimicrobial agents and chemotherapy, 50 (2006) 1615-1622.
[12] D.-H. Kwon, C.-D. Lu, Polyamine Effects on Antibiotic Susceptibility in Bacteria, Antimicrobial Agents and Chemotherapy, 51 (2007) 2070.
[13] O.M. El-Halfawy, M.A. Valvano, Putrescine reduces antibiotic-induced oxidative stress as a mechanism of modulation of antibiotic resistance in Burkholderia cenocepacia, Antimicrobial agents and chemotherapy, 58 (2014) 4162-4171.
[14] M. Goytia, W.M. Shafer, Polyamines Can Increase Resistance of Neisseria gonorrhoeae to Mediators of the Innate Human Host Defense, Infection and Immunity, 78 (2010) 3187.
[15] P. Koski, M. Vaara, Polyamines as constituents of the outer membranes of Escherichia coli and Salmonella typhimurium, J Bacteriol, 173 (1991) 3695-3699.
[16] A.L. Dela Vega, A.H. Delcour, Polyamines decrease Escherichia coli outer membrane permeability, J Bacteriol, 178 (1996) 3715-3721.
[17] S.K. Ballas, N. Mohandas, L.J. Marton, S.B. Shohet, Stabilization of erythrocyte membranes by polyamines, Proc Natl Acad Sci U S A, 80 (1983) 1942-1946.
[18] F. Schuber, Influence of polyamines on membrane functions, Biochem J, 260 (1989) 1-10.
[19] R. Lakshminarayanan, W.X. Tan, T.T. Aung, E.T.L. Goh, N. Murugananthan, J. Li, J.Y.T. Chang, N. Dikshit, P. Saraswathi, R.R. Lim, T.S. Kang, V. Balamuralidhar, B. Sukumaran, C.S. Verma, J. Sivaraman, S.S. Chaurasia, S. Liu, R.W. Beuerman, Branched Peptide, B2088, Disrupts the Supramolecular Organization of Lipopolysaccharides and Sensitizes the Gram-negative Bacteria, Sci Rep, 6 (2016) 25905-25905.
[20] F.J.S. Pontes, V.H. Rusu, T.A. Soares, R.D. Lins, The Effect of Temperature, Cations, and Number of Acyl Chains on the Lamellar to Non-Lamellar Transition in Lipid-A Membranes: A Microscopic View, Journal of Chemical Theory and Computation, 8 (2012) 3830-3838.
[21] E.T. Rietschel, H.-W. Wollenweber, U. Zähringer, O. Lüderitz, Lipid A, the lipid component of bacterial lipopolysaccharides: Relation of chemical structure to biological activity, Klinische Wochenschrift, 60 (1982) 705-709.
[22] T. Wei, T. Huang, B. Qiao, M. Zhang, H. Ma, L. Zhang, Structures, Dynamics, and Water Permeation Free Energy across Bilayers of Lipid A and Its Analog Studied with Molecular Dynamics Simulation, The Journal of Physical Chemistry B, 118 (2014) 13202-13209.

[23] S. Kim, D.S. Patel, S. Park, J. Slusky, J.B. Klauda, G. Widmalm, W. Im, Bilayer Properties of Lipid A from Various Gram-Negative Bacteria, Biophys J, 111 (2016) 1750-1760.
[24] D.C. Morrison, D.M. Jacobs, Binding of polymyxin B to the lipid A portion of bacterial lipopolysaccharides, Immunochemistry, 13 (1976) 813-818.
[25] L.A. Clifton, M.W.A. Skoda, A.P. Le Brun, F. Ciesielski, I. Kuzmenko, S.A. Holt, J.H. Lakey, Effect of divalent cation removal on the structure of gram-negative bacterial outer membrane models, Langmuir, 31 (2015) 404-412.
[26] A. Rice, J. Wereszczynski, Atomistic Scale Effects of Lipopolysaccharide Modifications on Bacterial Outer Membrane Defenses, Biophys J, 114 (2018) 1389-1399.
[27] M. Vaara, Agents that increase the permeability of the outer membrane, Microbiol Rev, 56 (1992) 395-411.
[28] C. Oostenbrink, T.A. Soares, N.F.A. van der Vegt, W.F. van Gunsteren, Validation of the 53A6 GROMOS force field, European Biophysics Journal, 34 (2005) 273-284.
[29] I.G. Tironi, R. Sperb, P.E. Smith, W.F.v. Gunsteren, A generalized reaction field method for molecular dynamics simulations, The Journal of Chemical Physics, 102 (1995) 5451-5459.
[30] M. Stroet, B. Caron, K.M. Visscher, D.P. Geerke, A.K. Malde, A.E. Mark, Automated Topology Builder Version 3.0: Prediction of Solvation Free Enthalpies in Water and Hexane, Journal of Chemical Theory and Computation, 14 (2018) 5834-5845.
[31] A.D. Mackerell Jr, Empirical force fields for biological macromolecules: Overview and issues, Journal of Computational Chemistry, 25 (2004) 1584-1604.
[32] B. Hess, H. Bekker, H.J.C. Berendsen, J.G.E.M. Fraaije, LINCS: A linear constraint solver for molecular simulations, Journal of Computational Chemistry, 18 (1997) 1463-1472.
[33] P. Bjelkmar, P. Larsson, M.A. Cuendet, B. Hess, E. Lindahl, Implementation of the CHARMM Force Field in GROMACS: Analysis of Protein Stability Effects from Correction Maps, Virtual Interaction Sites, and Water Models, Journal of Chemical Theory and Computation, 6 (2010) 459-466.
[34] T. Katsu, H. Nakagawa, K. Yasuda, Interaction between polyamines and bacterial outer membranes as investigated with ion-selective electrodes, Antimicrobial agents and chemotherapy, 46 (2002) 1073-1079.
[35] I. Szleifer, D. Kramer, A. Ben-Shaul, D. Roux, W.M. Gelbart, Curvature Elasticity of Pure and Mixed Surfactant Films, Physical Review Letters, 60 (1988) 1966-1969.
[36] M.J. Stevens, Coarse-grained simulations of lipid bilayers, The Journal of Chemical Physics, 121 (2004) 11942-11948.
[37] D.E.S. Santos, L. Pol-Fachin, R.D. Lins, T.A. Soares, Polymyxin Binding to the Bacterial Outer Membrane Reveals Cation Displacement and Increasing Membrane Curvature in Susceptible but Not in Resistant Lipopolysaccharide Chemotypes, Journal of Chemical Information and Modeling, 57 (2017) 2181-2193.
[38] L. Johnson, H. Mulcahy, U. Kanevets, Y. Shi, S. Lewenza, Surface-localized spermidine protects the Pseudomonas aeruginosa outer membrane from antibiotic treatment and oxidative stress, J Bacteriol, 194 (2012) 813-826.
[39] A. Anandan, G.L. Evans, K. Condic-Jurkic, M.L. O'Mara, C.M. John, N.J. Phillips, G.A. Jarvis, S.S. Wills, K.A. Stubbs, I. Moraes, C.M. Kahler, A. Vrielink, Structure of a lipid A phosphoethanolamine transferase suggests how conformational changes govern substrate binding, Proceedings of the National Academy of Sciences, 114 (2017) 2218.
[40] Y.-Y. Liu, C.E. Chandler, L.M. Leung, C.L. McElheny, R.T. Mettus, R.M.Q. Shanks, J.-H. Liu, D.R. Goodlett, R.K. Ernst, Y. Doi, Structural Modification of Lipopolysaccharide Conferred by mcr-1 in Gram-Negative ESKAPE Pathogens, Antimicrobial Agents and Chemotherapy, 61 (2017) e00580-00517.

[41] Y.-Y. Liu, Y. Wang, T.R. Walsh, L.-X. Yi, R. Zhang, J. Spencer, Y. Doi, G. Tian, B. Dong, X. Huang, L.-F. Yu, D. Gu, H. Ren, X. Chen, L. Lv, D. He, H. Zhou, Z. Liang, J.-H. Liu, J. Shen, Emergence of plasmid-mediated colistin resistance mechanism MCR-1 in animals and human beings in China: a microbiological and molecular biological study, The Lancet Infectious Diseases, 16 (2016) 161-168.
[42] H. Khalil, T. Chen, R. Riffon, R. Wang, Z. Wang, Synergy between Polyethylenimine and Different Families of Antibiotics against a Resistant Clinical Isolate of Pseudomonas aeruginosa, Antimicrobial Agents and Chemotherapy, 52 (2008) 1635-1641.
[43] K. Yasuda, C. Ohmizo, T. Katsu, Mode of action of novel polyamines increasing the permeability of bacterial outer membrane, International Journal of Antimicrobial Agents, 24 (2004) 67-71.

Declaration of interests

☒ The authors declare that they have no known competing financial interests or personal relationships that could have appeared to influence the work reported in this paper.

☐The authors declare the following financial interests/personal relationships which may be considered as potential competing interests: